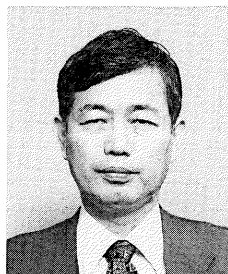


**A FUNDAMENTAL STUDY ON PROPAGATION BEHAVIOR
OF ELASTIC WAVES IN CONCRETE**

(Translation from Proceeding of JSCE, No.627/V-44, August 1999)



Mitsuyasu IWANAMI



Nobuaki OTSUKI



Junichiro NIWA



Toshiro KAMADA



Shigeyoshi NAGATAKI

In this study, the propagation behavior of elastic waves in concrete is investigated through both experimental and theoretical approaches. The size and quantity of aggregate in concrete are found to be key factors affecting the propagation behavior of elastic waves. Furthermore, it is clarified that the pulse velocity relates to the characteristics of the cement-paste matrix. In addition, the state of the aggregate-matrix interfaces and the presence of microcracks affect the frequency characteristics of elastic waves propagating through concrete.

Keywords: concrete, elastic waves, velocity, frequency, scattering

Mitsuyasu Iwanami is a researcher of the Port and Harbour Research Institute, Ministry of Transport, Japan. He received his Doctor of Engineering Degree from Tokyo Institute of Technology in 1999. His research interests are related to maintenance techniques for port and harbour facilities and nondestructive testing of concrete structures.

Nobuaki Otsuki is a professor of civil engineering at Tokyo Institute of Technology. He received his Doctor of Engineering Degree from Tokyo Institute of Technology in 1986. His research interests include durability and rehabilitation of reinforced concrete structures.

Junichiro Niwa is a professor of civil engineering at Tokyo Institute of Technology. He received his Doctor of Engineering Degree from the University of Tokyo in 1983. He has served as Secretary of the Concrete Committee of the JSCE from April 1999. He specializes in the mechanics of structural concrete including fracture mechanics, shear problems, and the application of FEM analysis.

Toshiro Kamada is an associate professor of civil engineering at Gifu University, Japan. He received his Doctor of Engineering Degree from Tokyo Institute of Technology in 1997. His main research work has been on nondestructive testing of concrete structures.

JSCE and ACI Fellow Shigeyoshi Nagataki is a professor emeritus of civil engineering at Tokyo Institute of Technology, and a professor of civil engineering and architecture at Niigata University, Japan. He received his Doctor of Engineering Degree from the University of Tokyo in 1966. His research interests cover physical and chemical properties of concrete, durability of concrete, effective utilization of additives, nondestructive testing, and recycling of concrete. He was awarded JSCE Yoshida prizes three times in 1972, 1987, and 1989, and JSCE thesis prize two times in 1991 and 1998.

1. INTRODUCTION

The importance of properly maintaining concrete structures has recently come to be widely recognized, and as a consequence nondestructive evaluation techniques for concrete deterioration are being studied and developed. Such techniques provide essential information for the prediction of future deterioration of concrete structures as they allow the collection of time-history data regarding damages in concrete structures.

Among the various nondestructive testing methods, techniques using elastic waves are considered particularly effective for rational maintenance because of their ease of use. Some methods based on elastic waves have been already proposed, including a method for measuring crack depth in concrete [1], a method for estimating concrete strength [2], a method for evaluating material deterioration in concrete [3], and others. In these methods, the characteristics of elastic waves propagating through concrete, such as velocity and frequency distribution, are employed as an evaluation index. As a result, it is of great importance to comprehend how the deterioration or defects in concrete affect the propagation behavior of elastic waves. However, the propagation behavior of elastic waves in concrete has not yet been clarified thoroughly although some efforts [4] have been made in recent decades. Consequently, the results obtained using elastic wave methods have low confidence, and cannot be relied on under such ambiguous conditions.

Although the propagation behavior of elastic waves in concrete is extremely complex, the ingredients of concrete, that is, cement paste and aggregate, are thought to be homogenous. The authors treat concrete as a composite material in which aggregate particles are dispersed randomly within a homogenous cement paste matrix, and investigate the propagation behavior of elastic waves in this composite material. Various inhomogeneities in the composite material add complexity to the propagation behavior, so the velocity and frequency characteristics of the elastic waves change drastically with changes in material properties. It is assumed that the following three factors have particularly strong influences on the velocity and frequency characteristics of elastic waves in concrete: the existence of aggregate, the properties of cement paste matrix, and the existence of microcracks

In this study, the influence of these three factors on the velocity and frequency characteristics of elastic waves propagating through concrete is investigated both experimentally and theoretically.

First, in order to understand the characteristics of elastic wave propagation behavior in a composite material like concrete, some tests were conducted with model specimens. These specimens consisted of cement paste and model aggregate of varying diameter, quantity and material characteristics. Furthermore, a theoretical investigation was carried out on the basis of the research on the elastic modulus of particle-dispersion-type composite materials and a formulation of scattering of elastic waves due to spherical inclusions.

Next, similar experiments were performed using specimens with actual aggregate in order to examine the influence of maximum size, shape, quantity and interfacial conditions of aggregate on the propagation behavior of elastic waves in concrete.

Finally, the influence of two other factors, the properties of cement paste matrix and the existence of microcracks, on the velocity and frequency distribution of elastic waves propagating through concrete was investigated.

2. FUNDAMENTAL INVESTIGATION OF PROPAGATION BEHAVIOR OF ELASTIC WAVES USING MODEL SPECIMENS

In order to obtain basic knowledge about the propagation behavior of elastic waves in a particle-dispersion-type composite material such as concrete, investigations were conducted with specimens in which glass or steel balls were used as model aggregate. In these experiments, the influence of changes in diameter, quantity, and material of the model aggregate was examined with respect to the velocity and frequency characteristics of elastic waves in the model specimens. Moreover, the experimental results were confirmed using a theoretical approach based on previous works related to the elastic modulus of particle-dispersion-type composite materials and the scattering characteristics of elastic waves due to spherical inclusions.

2.1 Outline of Experiment

a) Specimens

The specimens used for this investigation were fabricated from cement paste and model aggregate. The size of the specimens was 100x100x200(mm). The water to cement ratio (hereinafter referred as W/C) of the cement paste was set at 0.30 so as to ensure that the fresh concrete had sufficient viscosity to prevent a sinking of aggregate due to segregation.

The model aggregate consisted of glass balls, which had almost the same acoustical impedance as actual aggregate, and steel balls to investigate a case where the aggregate have a quite different acoustical impedance. Here, the acoustical impedance is defined as the product of density and velocity for a material in which elastic waves propagate. The acoustical impedance of glass balls and steel balls was $13.1 \times 10^6 \text{ kg/m}^2\text{s}$ and $46.8 \times 10^6 \text{ kg/m}^2\text{s}$, respectively. The range of acoustical impedance for ordinary actual aggregate is $10\text{-}15 \times 10^6 \text{ kg/m}^2\text{s}$. The acoustical impedance of the cement paste used in this experiment was $9.58 \times 10^6 \text{ kg/m}^2\text{s}$.

In order to investigate the influence of aggregate size and quantity on the propagation behavior of elastic waves, glass balls of diameter 12mm, 20mm, and 30mm were used, and the quantity of model aggregates was made 10%, 25%, and 35% by volume.

By using specimens with different acoustical impedance, the influence of acoustical impedance differential between matrix and aggregates can be examined. Taking the acoustical impedance of the cement paste matrix as 1, the acoustical impedance of the glass and steel balls was 1.36 and 4.89, respectively. In this case, the diameter and volume ratio of the steel balls was fixed at 13mm and 25%, respectively.

b) Outline of elastic wave propagation test

The elastic wave measurement system is shown in Fig.1. A pulse was produced by a wide-range ultrasonic probe and received by a wide-range AE sensor after propagating through a specimen. The width of the incident pulse was $0.8 \mu\text{s}$, and the input voltage was 65V. The analog waveform received by the AE sensor was digitized using an A/D converter with a sampling frequency of 2MHz. This data was stored in a personal computer for analysis. Ultimately, the velocity and frequency distribution of the

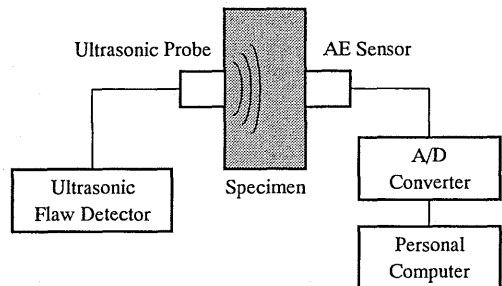


Fig.1 Elastic Waves Measurement System

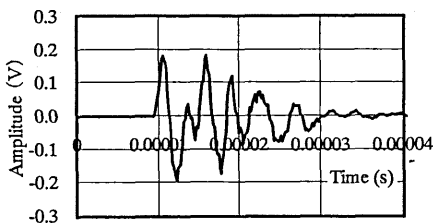


Fig.2 Waveform Propagating Through Aluminum

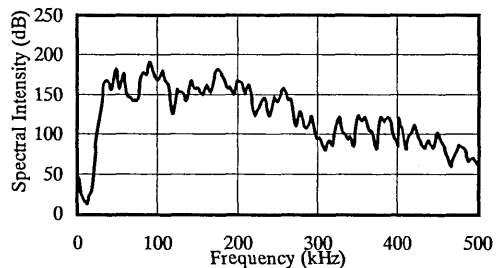


Fig.3 Frequency Distribution of Incident Waves

elastic waves were calculated and used as evaluation indices. The frequency distribution was obtained by an FFT procedure.

The surface and moisture conditions of the concrete specimens are very influential on these measurements. Details of the treatment applied to ensure consistency are as follows. The surface of the specimens was ground and greased, and the moisture conditions were controlled to be saturated surface dry.

It was of great importance to clarify the characteristics of the incident waves. The waveform of a pulse transmitted through an aluminum plate 100mm in thickness and its frequency distribution are shown in Fig.2 and Fig.3, respectively. It is believed that losses through this aluminum plate are negligible compared with those in concrete, so the results obtained with this aluminum plate can be treated as the waveform and frequency distribution of the incident waves. From Fig.3, it is confirmed that the incident pulse has a very wide frequency distribution of 0-500kHz.

2.2 Experimental Results and Discussion

a) Influence of size and quantity of model aggregate on elastic wave velocity

In Fig.4, the influence of diameter, and in Fig.5, the influence of volume ratio, of model aggregate on the velocity of elastic waves propagating through model specimens are shown, respectively. From these figures, it can be seen that the influence of volume ratio is much larger than that of diameter. This is because a higher content of aggregate, which has a higher velocity than the cement paste matrix, results in a higher velocity for the composite material as a whole, as seen in Table 1.

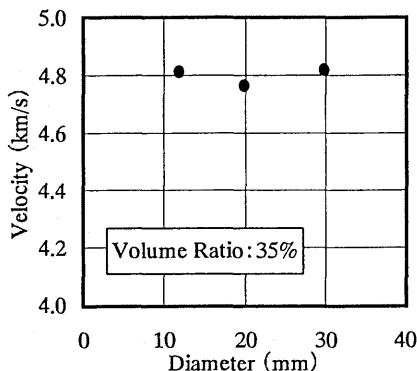


Fig.4 Relationship Between Velocity and Diameter of Model Aggregate

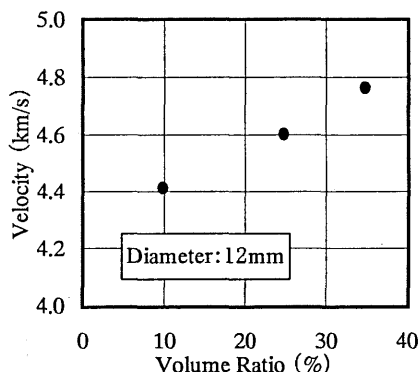


Fig.5 Relationship Between Velocity and Quantity of Model Aggregate

b) Influence of size and quantity of model aggregate on frequency characteristics

The influence of diameter and volume ratio of model aggregates on the frequency distribution of elastic waves propagating through model specimens are shown in Fig.6 and Fig.7, respectively. From these figures, it is clear that the larger the diameter or the greater the volume ratio of model aggregate, the lower in amplitude the high-frequency components become.

This attenuation was observed particularly clearly in the frequency range 200-400kHz, which is a wavelength equivalent to the model aggregates' diameter. From this observation, it is concluded that this attenuation of elastic waves is caused by scattering from model aggregate.

To compare the influence of diameter and volume ratio of model aggregate on the attenuation, an index that we call "average frequency" was defined as in Equation(1).

Table 1 Properties of Materials Used

Material	Density (g/cm ³)	Velocity (km/s)	Poisson's Ratio
Cement Paste (W/C=0.3)	2.21	4.33	0.242
Glass Ball	2.50	5.60	0.200
Steel Ball	7.86	5.95	0.300
Cement Paste (W/C=0.5)	1.97	3.72	0.265
Aggregate	2.61	5.63	0.200

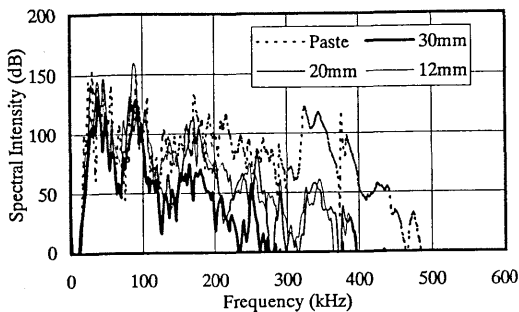


Fig.6 Frequency Distributions for Different Diameters

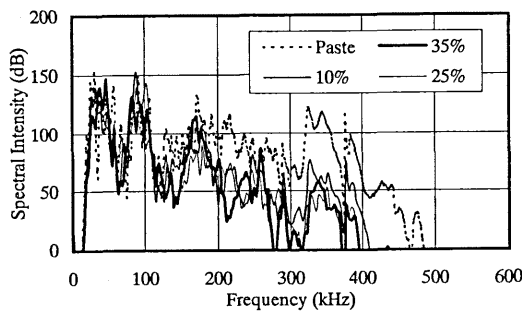


Fig.7 Frequency Distributions for Different Quantities of Model Aggregate

$$f_{ave} = \frac{\int f \cdot S(f) df}{\int S(f) df} \quad (1)$$

where, f : frequency; and $S(f)$: spectral intensity at f . This index of average frequency represents the center of gravity of the frequency distribution and its value decreases when components in high-frequency region is attenuated, as illustrated in Fig.8. The influence of diameter and of volume ratio of the model aggregate on the average frequency are shown in Fig.9 and Fig.10, respectively. Comparing these two figures, it can be recognized that the diameter has a greater influence on the frequency characteristics of elastic waves within the limit of this study.

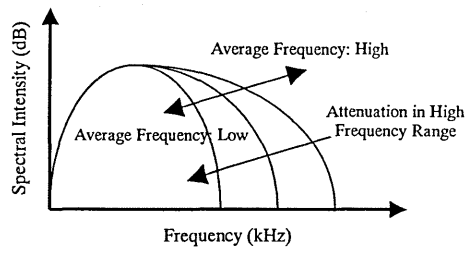


Fig.8 Average Frequency

c) Examination of influence of acoustical impedance

The velocity of elastic waves propagating through specimens with glass balls and steel balls (12mm in diameter and 25% in volume ratio) was 4.42km/s and 4.60km/s, respectively. This difference arises because the velocity of steel itself is larger than that of glass.

Next, the frequency distributions for these two cases are shown in Fig.11. Looking at the higher frequency region, the attenuation for steel balls is more notable than that for glass balls. The reason for this is the larger acoustical impedance differential between matrix and aggregate, which leads to greater scattering of elastic waves at their boundary, as explained in the next section. As to the acoustical impedance of the aggregate, it can be said that the

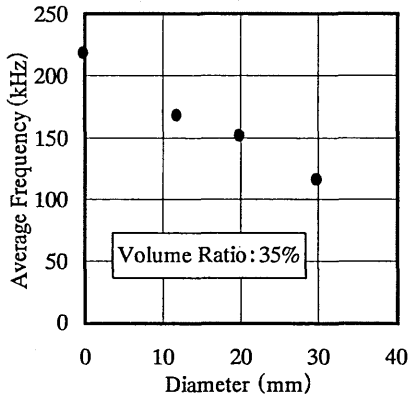


Fig.9 Relationship Between Average Frequency and Diameter of Model Aggregate

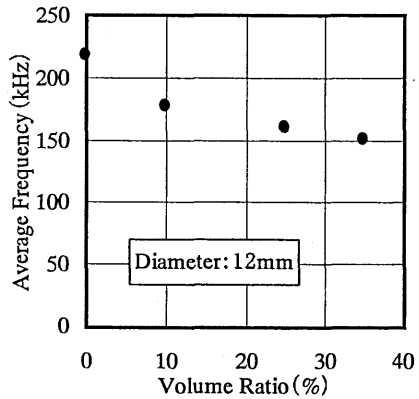


Fig.10 Relationship Between Average Frequency and Quantity of Model Aggregate

greater its difference from that of the matrix then the more significant the attenuation in the high-frequency region. In theory, the influence of the interfacial transition zone between matrix and aggregate (hereafter referred as ITZ) should be also taken into account because the bonding conditions of each type of aggregate might be different. However, in this section, the influence of ITZ was neglected, assuming complete bonding between the matrix and aggregate.

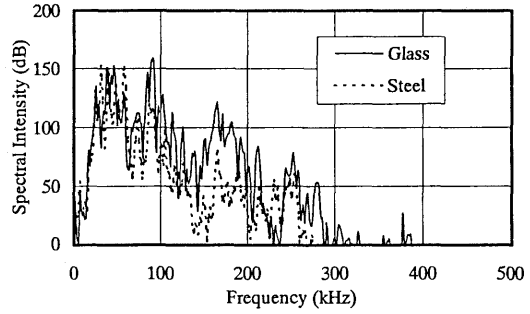


Fig.11 Frequency Distributions for Different Materials of Model Aggregate

2.3 Theoretical Consideration

a) Examination of elastic wave velocity

Theoretically, the velocity of elastic waves can be calculated by the following equation [5].

$$V = \sqrt{\frac{E(1-\nu)}{\rho(1+\nu)(1-2\nu)}} \quad (2)$$

where, E : elastic modulus; ρ : density; and ν : Poisson's ratio.

Thus, the velocity of the elastic waves can be obtained from a data set consisting of E, ρ , and ν for the material under consideration. In the calculations in this section, the specimen used was assumed to be a 2-phase composite material [6].

There are four equations which relate K, K_0 , K_1 , G, G_0 , G_1 , E, and ν .

$$\frac{K}{K_0} = 1 + \frac{r}{\frac{3(1-\nu)K_0}{3K_0 + 4G_0} + \frac{K_0}{K_1 - K_0}} \quad (3)$$

$$\frac{G}{G_0} = 1 + \frac{r}{\frac{6(1-\nu)(K_0 + 2G_0)}{5(3K_0 + 4G_0)} + \frac{G_0}{G_1 - G_0}} \quad (4)$$

$$K = \frac{E}{3(1-2\nu)} \quad (5)$$

$$G = \frac{E}{2(1+\nu)} \quad (6)$$

where, K, G : volume elastic coefficient and stiffness of 2-phase composite material; K_0 , G_0 : those of matrix; K_1 , G_1 : those of inclusions; and r : volume ratio of inclusions.

So, if K_0 , K_1 , G_0 , G_1 , and r are given, E and ν for the 2-phase composite material can be calculated from Equations(3) to (6). To calculate K_0 , K_1 , G_0 , and G_1 for each material (cement paste, glass balls, and steel balls), the longitudinal wave velocity V_p (usually referred as elastic wave velocity V), ρ , and ν should be known. Then, using Equation(7) below, the shear wave velocity V_s can be calculated.

$$V_s = \sqrt{\frac{1-2\nu}{2(1+\nu)}} V_p \quad (7)$$

From these values of V_p and V_s , values of K and G can be calculated with Equations(8) and (9).

$$\frac{3K + 4G}{3} = \rho \cdot V_p^2 \quad (8)$$

$$G = \rho \cdot V_s^2 \quad (9)$$

Hence, the elastic wave velocity through a specimen containing model aggregate can be calculated with Equation(2) using the values of V , ρ , and v for each ingredient.

The relationship between values calculated by this method and the measured values is shown in Fig.12. This figure confirms the validity of this theory and also the larger influence of volume ratio on the velocity. Consequently, concrete may be treated as a 2-phase composite material in which the particles are dispersed randomly in a uniform matrix.

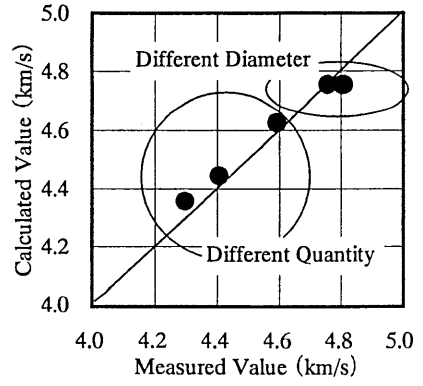


Fig.12 Relationship Between Measured Velocity and Calculated Velocity

b) Examination of frequency characteristics

To investigate the influence of diameter and volume ratio on the propagation behavior of elastic waves in concrete, a model of elastic wave scattering is introduced as shown in Fig.13. This model is a very simple one in which only one inclusion exists in an infinite homogeneous matrix. In this case, the ratio of the amplitude of scattered waves at P to that of the incident waves, ξ_r/ξ_a , is theoretically given by Rayleigh [7], as shown in Equation(10). In this equation, it is assumed that the matrix is uniform, and that the wavelength is smaller than the diameter of inclusions.

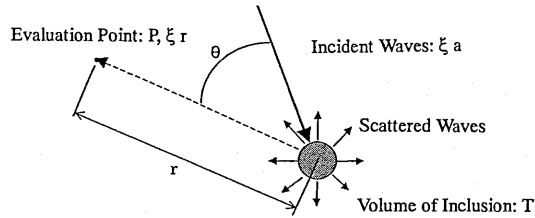


Fig.13 Scattering of Elastic Waves

$$\frac{\xi_r}{\xi_a} = \frac{\pi T}{r\lambda^2} \left(\frac{K_1 - K_0}{K_0} + \frac{\rho_1 - \rho_0}{\rho_0} \cos\theta \right) \quad (10)$$

where, λ : wavelength; ρ_0 , ρ_1 : density of matrix, inclusions; K_0 , K_1 : acoustical impedance of matrix, inclusions; and T : volume of inclusions.

With this equation, the attenuation coefficient of elastic waves can be obtained according to Mason [8] as shown in Equation(11). In this equation, the effect of multiple scattering is neglected and the particles are randomly arranged in three-dimensional space.

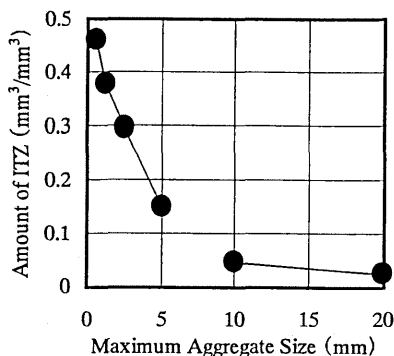


Fig.18 Relationship Between Amount of ITZ and Maximum Aggregate Size

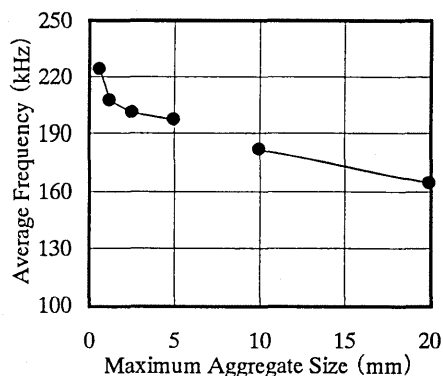


Fig.19 Relationship Between Average Frequency and Maximum Aggregate Size

where, S : specific surface area; ρ : density of aggregate; and d : diameter of aggregate.

As shown in Fig.18, the smaller the maximum aggregate size, the more ITZ present in the concrete, resulting in a lower elastic wave velocity. Thus, the existence of ITZ is one of the reasons for the difference between measured velocity and the theoretical value.

Fig.19 shows the relationship between maximum aggregate size and average frequency defined as in Equation(1). From this figure, it is clear that the larger the maximum aggregate size, the lower the average frequency. This tendency is identical to that observed in the case of the model aggregate.

3.2 Examination of Aggregate Shape

a) Outline of specimens

To examine the influence of aggregate shape, specimens were fabricated with crushed rock and compared with the gravel case appeared in the previous section. The maximum size and particle size distribution of the crushed rock were controlled to be equivalent to those of the gravel. The other materials used were the same as previously described, as illustrated in Table 4. As shown in this table, characteristics such as density, water absorption ratio, etc, of both coarse aggregates were quite similar. Furthermore, the both coarse aggregates came from the same river system. Therefore, the acoustical characteristics of these aggregates can be assumed to be identical except for their shape. The mixture proportion is shown as in No.3 in Table 3. The specimen dimensions were 100x200x200(mm).

b) Experimental results and discussion

Fig.20 shows the velocity and average frequency of elastic waves propagating through concrete with the different types of coarse aggregate. Since the bonding conditions were different because of differences in specific surface area and surface roughness of the aggregate, it was presumed that there would be a difference in propagation behavior of elastic waves between crushed rock concrete and gravel concrete. However, the discrepancy actually observed with regard to the velocity and average frequency was rather small. Therefore, it was concluded that the aggregate shape had little influence on the propagation behavior of elastic waves in concrete.

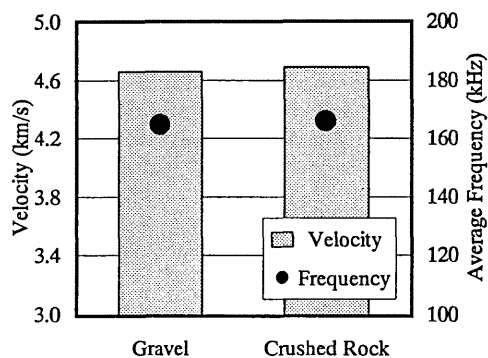


Fig.20 Test Results for Different Aggregate Shape

3.3 Examination of Aggregate Quantity

a) Outline of specimens

In this section, the volume ratio of coarse aggregate was made 55%, 68%, and 78% to clarify the influence of this parameter. W/C of the concrete was 0.50 and the maximum aggregate size was 20mm. The mixture proportions were Nos.3-5 in Table 3, and the materials used were the same as those given in the previous section, as shown in Table 4. An anti-segregation agent and a superplasticizer were added during mixing to obtain appropriate workability and segregation resistance in the case of 55% and 78% aggregate content, respectively. The specimens were 100x200x200(mm) prisms. Three specimens were prepared for each case.

b) Experimental results and discussion

The change in elastic wave velocity with volume ratio of aggregate is shown in Fig.21. The theoretical values calculated as in Chapter2 are also plotted in this figure. It can be seen that the larger the volume ratio, the larger the velocity. This tendency is similar to the case of model aggregate and the theoretical calculations. Further, this range of the velocities was larger than that for the maximum aggregate size, as mentioned in the section of 3.1. The difference between experimental and theoretical values increased with the falling in aggregate quantity. The reason for this is thought to be related to the ITZ volume in the concrete. That is, the lower the volume ratio of aggregate, the higher the unit water content of concrete and the more remarkable the amount of bleeding, increasing the ITZ volume.

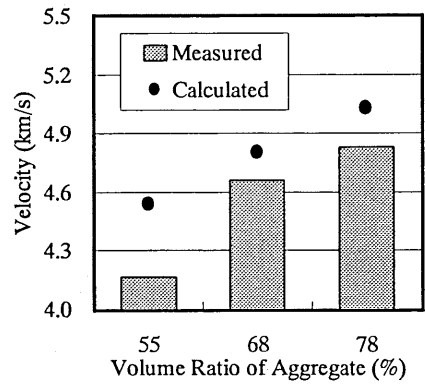


Fig.21 Relationship Between Velocity and Aggregate Quantity

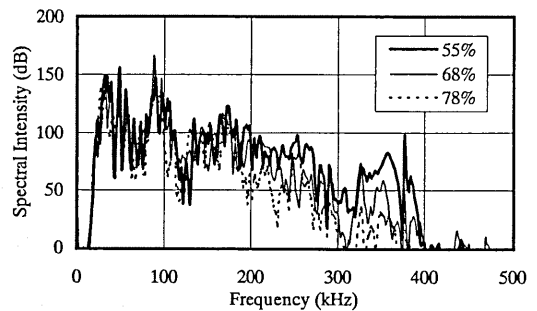


Fig.22 Frequency Distributions for Different Quantities of Aggregate

The frequency distribution of elastic waves for each volume ratio is shown in Fig.22. It can be observed that the reduction in spectral intensity at frequencies above 200kHz is more pronounced as the volume ratio of aggregate becomes larger. This is because the scattering of elastic waves becomes more prominent with increasing aggregate quantity. This tendency reflects that of the model aggregate.

From these results, it is clear that the volume ratio of aggregate influences the frequency characteristics of elastic waves propagating through concrete as well as their velocity.

3.4 Examination of Interfacial Properties Between Matrix and Aggregate

It is known that there exists interfacial transition zone (ITZ) around aggregate particles in concrete. The porosity of ITZ is much higher than that of the bulk of matrix, resulting in a weak point from the viewpoint of mechanical performance. Furthermore, it forms a channel for harmful substances to penetrate through the concrete. It is also assumed that the existence of ITZ affects the propagation behavior of elastic waves in concrete. In this section, several specimens are fabricated and tested with artificially adjusted conditions of the interfaces between matrix and aggregate. The aim is to clarify the influence of ITZ on the velocity and frequency characteristics of elastic waves.

a) Outline of specimens

Three specimens 100x200x200(mm) in size were used for each test condition in this experiment. In order to obtain different bonding conditions between matrix and aggregate, the following four types of concrete specimens were prepared:

1. crushed rock was used as coarse aggregate (referred as the normal case)
2. 40% of cement by weight was replaced by blast furnace slag powder (referred as the BFS case)
3. crushed rock pre-coated with cement paste [12] was used as coarse aggregate (referred as the coated case)
4. crushed rock covered with machine oil was used as coarse aggregate (referred as the oil case)

In the BFS case, it was hard for ITZ to form around aggregate particles as a result of the effect of latent hydration of BFS, which considerably reduces the amount of $\text{Ca}(\text{OH})_2$ around aggregate particles [13].

The maximum size and volume ratio of aggregate was fixed at 20mm and 68%, respectively. In order to obtain consistent cement paste matrix characteristics, W/C for all types of concrete was 0.50, except in the BFS case. The addition of BFS into concrete changes the cement paste matrix properties. Therefore, W/C in this case was set to be 0.55 to ensure that the compressive strength of the BFS cement paste was equal to that of the other cases.

In the coated case, crushed rock particles were pre-coated with W/C=0.40 cement paste before making the specimens. The pre-coating thickness was about 0.25mm, as estimated from the volume of cement paste used for pre-coating and the specific surface area of the aggregate as calculated on the assumption that the particles were spherical. In mixing this type of concrete, the amount of cement paste used for pre-coating was taken into account to ensure the amount of matrix in the concrete was identical to that in other cases.

b) Evaluation of interfacial properties

In order to quantify the interfacial conditions between matrix and aggregate, microhardness was measured around aggregate particles in four types of concrete. These measurements were conducted at points 10mm, 30mm, and 50 μm below from the aggregate boundary. It was assumed that bonding around the lower part of an aggregate particle would vary easily due to the effect of bleeding. The measured range of 50 μm was determined based on a report related to the thickness of ITZ [11]. The maximum load and its duration time used for microhardness measurements were 0.01N and 10s, respectively.

Fig.23 shows the average value of microhardness measured for each case. From this figure, it was found that the average value of microhardness of the BFS case and the coated case were larger than that of the normal case, implying improved bonding. In the coated case in particular, the increase in microhardness was remarkable. On the other hand, the value of microhardness for the oil case was smaller than that in the normal case, indicating poorer interfacial bonding between matrix and aggregate. It was confirmed that the four cases studied in this experiment had different bonding conditions between matrix and aggregate.

c) Influence of interfacial properties on propagation behavior of elastic waves

Fig.23 also illustrates the velocity of elastic waves propagating through each type of concrete. This figure shows that the better the bonding conditions between matrix and aggregate, the larger the elastic wave velocity. This is thought to be related to the existence of ITZ. Good bonding between the matrix and aggregate causes the reduction of the ITZ volume in concrete, which has lower elastic wave velocity than that of the bulk matrix because of its higher porosity. In the coated case, the elastic wave velocity is higher since a pre-coating layer encloses aggregate particles, and this is denser than the bulk matrix. Within the limit of this study, the velocity of elastic waves varied by about 0.2km/sec due to variation in bonding conditions around aggregate particles. The experimental cases in this study included impractical ones compared with actual bonding in normal concrete. Therefore, it can be said that the influence of interfacial properties on the velocity would be much smaller in the case of existing concrete.

The frequency distributions of elastic waves propagating through concrete with different interfacial properties are shown in Fig.24. In the case of bad bonding, such as the oil case, the spectral intensity is attenuated completely

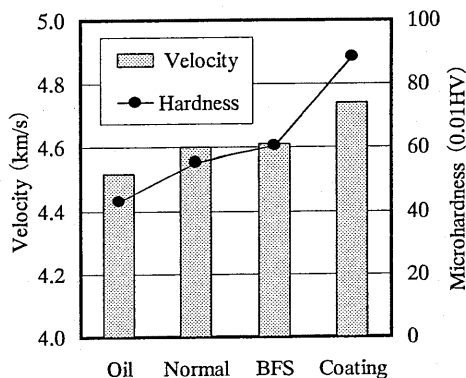


Fig.23 Relationship Between Velocity and Microhardness of ITZ

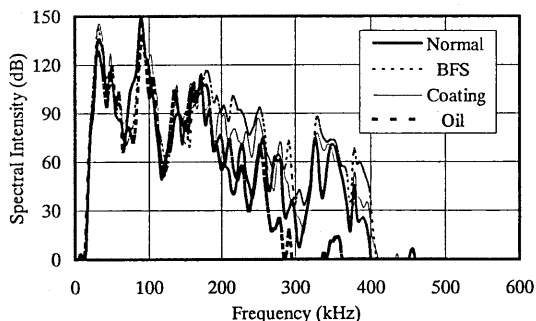


Fig.24 Frequency Distributions for Different Properties of ITZ

above 300kHz. On the other hand, good bonding conditions brought about a small increase in spectral intensity in the higher frequency range. Such differences in frequency characteristics originate from the difference in interfacial properties around the aggregate particles, and relate to the degree of scattering and reflection of elastic waves. The frequency range affected most by interfacial properties was 200-400kHz, and the corresponding wavelength is approximately 10-20mm. This coincides with the coarse aggregate size. From this, it is concluded that the attenuation shown in Fig.24 was caused by differences in interfacial properties around the aggregate particles.

4. INFLUENCE OF MATRIX PROPERTIES ON PROPAGATION BEHAVIOR OF ELASTIC WAVES

In the previous chapter, the influence of the existence of aggregate on the propagation behavior of elastic waves in concrete was investigated. Here, the influence of the other ingredients of concrete will be discussed on the basis of experimental results collected for specimens with different properties. In this chapter, W/C and air content of concrete are changed for the purpose of obtaining various cement paste matrix properties.

4.1 Outline of Specimens

Concrete block specimens 100x100x200(mm) in size were used in this experiment. Three specimens were prepared for each test case. W/C and air content of concrete were varied to obtain different cement paste matrix characteristics. In the series of tests with different W/C, W/C values were 0.30, 0.50 and 0.65 with the same quantity of aggregate. The mixture proportions are Nos.3, 6, and 7 in Table 3. In mixing the concrete, both workability and segregation resistance were kept appropriately by means of suitable chemical admixtures. A superplasticizer and an anti-segregation agent were used in the case of W/C=0.30 and 0.65, respectively.

In the series of tests with different air content, two types of concrete with air content of 6% were made to compare with the basic case of W/C=0.50 described above, in which the air content was 1%. One type had the same W/C as the basic case, and the another type had the same compressive strength as the basic case by setting W/C to be 0.42. The mixture proportions for this series were Nos.3, 8, and 9 in Table 3. The quantity of aggregate was constant in these concretes. In order to control air content of the concrete, an air-entraining agent was added as a chemical admixture. The properties of the materials used are shown in Table 4. Elastic wave propagation tests as in Chapter2 were conducted on specimens in this series.

4.2 Evaluation of Cement Paste Matrix Properties

In order to evaluate the properties of the cement paste matrix from the viewpoint of porosity, the index VR_p was employed as defined below. The total void content of concrete was assumed to be the difference in weight between two stage: one stage was after the voids in concrete were filled with water completely, and the other was after the concrete was heated in an electric oven 105 degrees centigrade in temperature until it attained constant weight. Some of the water evaporating during heating was from cement paste matrix, and the rest was from aggregate. The weight of water evaporating from aggregate was calculated using the void ratio of aggregate itself and the quantity of aggregate. Using this procedure, the weight of water removed only from the cement paste matrix could be estimated, and the index VR_p was calculated from Equation(13) as follows:

$$VR_p = \frac{M_w - (V_s \cdot VR_s + V_g \cdot VR_g)}{V_p} \times 100 \quad (13)$$

where, M_w : weight of water evaporating from concrete per unit volume; V_s, V_g, and V_p : volume ratios of fine aggregate, coarse aggregate, and cement paste; VR_s, VR_g : void ratios of fine aggregate and coarse aggregate (in this study, 0.0371 and 0.0258, respectively).

The value of VR_p calculated by this procedure includes the influence of ITZ.

4.3 Experimental Results and Discussion

Fig.25 shows the relationship between elastic wave velocity and VR_p as calculated from Equation(13) for both series: different W/C and different air content. It was found that there exists a strong correlation between elastic wave velocity and void content of cement paste matrix, regardless of W/C and air content. Within the limit of this study, the various properties of cement paste matrix caused about 1km/s change in velocity. A correlation such as that shown in Fig.25 exists only within the condition that the same quantity of aggregate is present in the concrete.

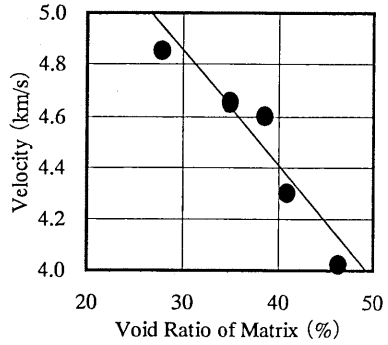


Fig.25 Relationship Between Velocity and Void Ratio of Matrix

Fig.26 shows frequency distributions for elastic waves propagating through the concrete with different W/C. From this figure, it is clear that the increase in W/C brings about considerable attenuation in the high-frequency range. Higher W/C concrete consists of cement paste matrix that is so porous that the acoustical impedance differential at matrix-aggregate interfaces became significant. As a result, the scattering and reflection of elastic waves at the interface became considerable. This corresponds to the result obtained with model specimens in which the aggregate material was varied; that is, when glass balls and steel balls were used in Chapter2.

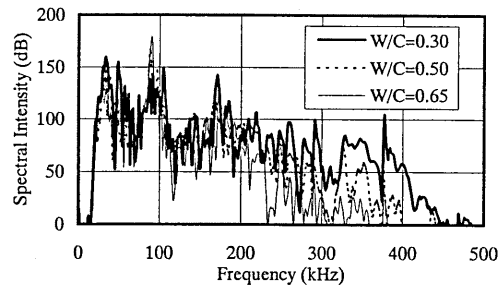


Fig.26 Frequency Distributions for Different W/C of Concrete

Next, the frequency distributions for different air content are shown in Fig.27. It is found that the higher frequency components are attenuated with increasing porosity of the cement paste matrix. This is thought to be caused by the differential in acoustical impedance between cement paste matrix and aggregate as well as by the different W/C described here.

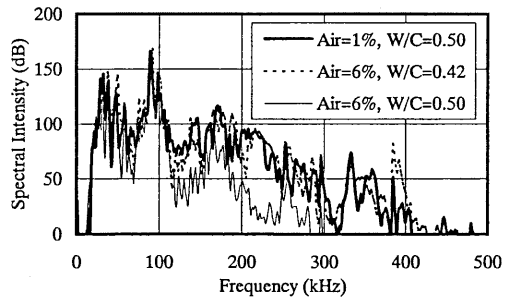


Fig.27 Frequency Distributions for Different Air Content of Concrete

5. INFLUENCE OF MICROCRACKS ON PROPAGATION BEHAVIOR OF ELASTIC WAVES

Microcracks occurs in concrete more or less due to the action of drying shrinkage, thermal stress, external loading, etc. Such discontinuities as microcracks are paths for detrimental substances to penetrate through concrete, and may also trigger more serious deterioration. Since the existence of microcracks in concrete is expected to be sources of scattering and reflection of elastic waves, the influence of microcracks on propagation behavior is investigated in this chapter.

5.1 Examination with Model Microcracks

In order to examine the influence of microcracks on the propagation behavior of elastic waves in concrete, specimens containing thin plastic pieces as model microcracks were manufactured. By conducting the elastic wave propagation tests as in Chapter2, the relationship between the amount of microcracks and the velocity and frequency characteristics of elastic waves propagating through concrete is determined.

a) Outline of specimens

The specimens were concrete cylinders 100mm in diameter and 200mm in height. The mixture proportion and the materials are shown as No.3 in Table 3 and Table 4, respectively. Three specimens were prepared for each experimental case.

The thin plastic pieces mixed into the concrete were 15x15x0.3(mm), and they were mixed at 0.5% and 1% by volume. Since this study focuses on interfacial microcracks between cement paste and aggregate particles, the artificial microcracks were sized in consideration of the maximum aggregate size of 20mm. The acoustical impedance of the plastic material used was 1-2kg/m²s, about 10% that of normal concrete.

b) Experimental results and discussion

Fig.28 shows the measured velocities of elastic waves with varying the amount of microcracks in the concrete. This figure shows that there is little change in velocity even if the amount of microcracks is increased to 1%. This is because the addition of plastic pieces into the concrete does not change the porosity of cement paste matrix. It also agrees with the results in Chapter4.

In Fig.29, the frequency distributions of elastic waves propagating through concrete containing different amounts of artificial microcracks are shown. It is found that higher frequency components are attenuated with increasing the quantity of model microcracks, which might act as scattering points for elastic waves. In particular, components above 300kHz, which correspond to the wavelength equivalent to the size of plastic pieces, decreased significantly. From this, it is confirmed that the attenuation noted here is caused by the existence of microcracks. Fig.28 demonstrates this attenuation in terms of average frequency as defined in Chapter2. This average frequency index is able to express the attenuation at higher frequencies; with more microcracks, the average frequency decreases.

From these results, it is concluded that the existence of discontinuities in concrete, such as microcracks, causes little change in the velocity of elastic waves, but they do attenuate higher- frequency components.

5.2 Examination with Actual Microcracks

In order to verify the results obtained with model microcracks described above, the authors made specimens with actual microcracks by prior loading, and examined their influence on the propagation behavior of elastic waves.

a) Outline of experiment

For the purpose of producing microcracks in concrete, prior loading was carried out on concrete specimens before elastic wave propagation tests. The load was applied in compression up to 20%, 40%, 60%, and 80% of the ultimate load, which had been measured in advance. A virgin specimen, which was not loaded, was prepared for comparison. The specimens were cylinders 100mm in diameter and 200mm in height. The mixture proportion and properties of the materials are as shown in No.3 in Table 3 and Table 4, respectively.

Visual observations of concrete specimen interiors were performed to evaluate the amount of microcracks caused by loading. After cutting a loaded specimen, the cut surface was soaked with a red dye. Polishing of the cut surface then made

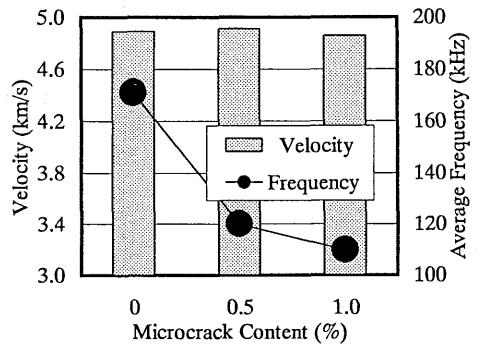


Fig.28 Test Results for Specimens Containing Model Microcrack

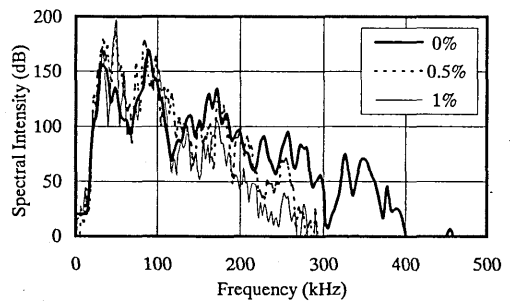


Fig.29 Frequency Distributions for Different Content of Microcrack

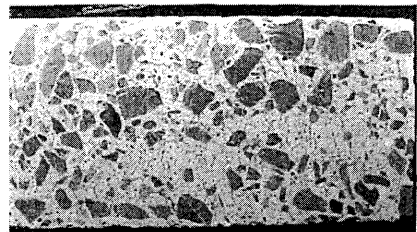


Photo.1 Example of Cut Surface

microcracks stand out as red lines. An example of a cut surface is shown in Photo.1. This is for a specimen loaded up to 80% of the ultimate load. The state of microcracking was elucidated from the red lines using an imaging analyzer. In this analysis, microcracks were classified into matrix-cracks and bond-cracks between matrix and aggregate. Crack density was employed as the evaluation index; it was defined as the ratio of the total length of microcracks to the area of cut surface. In theory, microcracks in the direction perpendicular to wave propagation should be chosen for this evaluation. However, as illustrated in Photo.1, microcracking was so random that the authors adopted the total length of microcracks as the index.

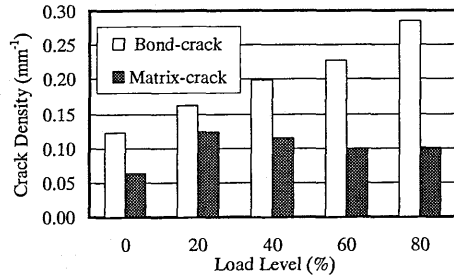


Fig.30 Results of Cross-sectional Observation

b) Evaluation of amount of microcracks in concrete

The amount of microcracks in concrete loaded up to the determined levels is shown in Fig.30 in terms of crack density. It is found that the amount of bond-cracks increased gradually with rising the load level, while there was little change in the amount of matrix-cracks. This means that these concrete specimens contained varying amount of bond-cracks between matrix and aggregates, while the matrix properties remained almost at their initial conditions. This coincides with the findings obtained in the previous section. Therefore, the propagation behavior of elastic waves is thought to be almost the same as that for concrete specimens with model microcracks. Incidentally, the few microcracks observed in the case of the virgin specimens are thought to be due to the existence of ITZ or the influence of cutting.

c) Propagation behavior of elastic waves in concrete containing actual microcracks

Fig.31 shows the changes in velocity and average frequency of elastic waves propagating through concrete loaded to various levels. Even when the amount of microcracks increased, no change in the velocity is observed. On the other hand, the frequency characteristics of the elastic waves are influenced by the existence of microcracks with the average frequency decreasing monotonically with applied load. This agrees well with the results obtained for concrete specimens containing plastic pieces as model microcracks, confirming the validity of the model microcracks. The change in average frequency in the case of actual microcracks was smaller than that in the case of model microcracks. This is because the surfaces of actual microcracks partially merged with each other, and because the thickness of actual microcracks was less than that of model microcracks.

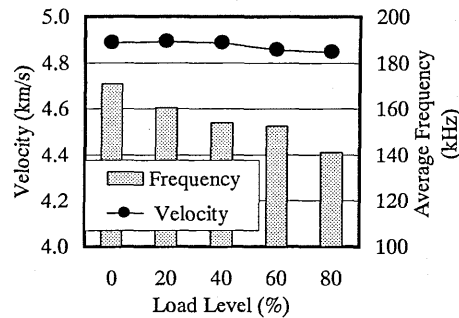


Fig.31 Influence of Microcracks on Propagation Behavior of Elastic Waves

d) Examination of microcrack thickness

The thickness of microcracks would change during loading and unloading, thus affecting the degree of scattering and reflection of elastic waves propagating through the concrete. For the purpose of clarifying this point, a comparison of elastic wave propagation behavior was carried out for loaded and unloaded case. The load level was set to 80% of the ultimate load, and the measurements were carried out at the same point on each specimen. The results are shown in Fig.32. From this figure, it is clear that the velocity did not change between loaded and unloaded. However, the average frequency for the loaded specimen, that is, with the microcracks opened up, was smaller than that for unloaded, demonstrating that greater scattering of elastic waves takes place. Therefore, the thickness of microcracks is a key factor in the frequency characteristics

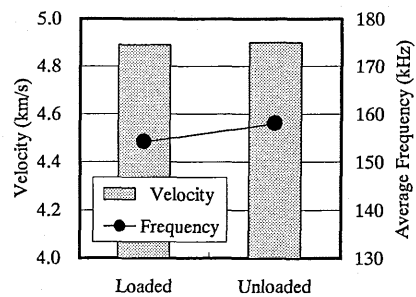


Fig.32 Influence of Microcracks Thickness on Propagation Behavior of Elastic Waves

of elastic waves propagating through concrete.

6. CONCLUSION

6.1 Summary of This Study

In this study, the influence of three factors among the various inhomogeneities of concrete on the propagation behavior of elastic waves was investigated: the presence of aggregate, the properties of cement paste matrix, and the presence of microcracks. The results obtained from experimental and theoretical analysis are summarized as follows:

1. The velocity of elastic waves is not influenced by aggregate size, but by the quantity of aggregate. With regard to frequency characteristics, attenuation at the higher frequency range becomes significant with larger aggregate. Furthermore, the validity of these findings was qualitatively confirmed through a theoretical approach.
2. There exists a strong correlation between elastic wave velocity and the porosity of cement paste matrix. Within the limit of this study, the variation in velocity was about 1km/s among cement paste matrixes with various properties. Since the matrix properties affect its acoustical impedance in accordance with the degree of scattering at matrix-aggregate interfaces, the frequency distribution of propagating waves also varies.
3. Microcracks and interfaces between matrix and aggregate have a great influence on the frequency characteristics of elastic waves propagating through concrete, but not on their velocity. This is because discontinuities in concrete, such as microcracks and interfaces, act as sources of scattering, causing attenuation at frequencies corresponding to a wavelength equal to the size of the discontinuities.

6.2 Conclusion Remarks

Considering the velocity and frequency characteristics of elastic wave propagating through concrete on the basis of these results, the following understanding has been obtained.

Within the limit of this study, the variation in velocity of elastic waves is about 1km/s and 0.2km/s according to changes in the matrix properties and the interfaces, respectively. It is therefore concluded that the influence of matrix-aggregate interfaces on the velocity was smaller than that of matrix properties. Since the range of interfacial conditions in this experiment was considerably wider than in actual practice, it can be assumed that the influence of matrix-aggregate interfaces under actual conditions would be yet smaller. Hence, the velocity of elastic waves is shown to be effective for evaluating matrix properties, such as porosity, and deterioration.

The existences of aggregate and microcracks in concrete have an influence on the frequency characteristics of elastic waves propagating through concrete, especially at higher frequencies. Therefore, it is better to use elastic waves of lower frequency for the purpose of accurate evaluation, thus removing the influence of aggregate and microcracks from the results. On the contrary, it would be helpful to pay attention to this attenuation at higher frequencies when the amount of microcracks in concrete is to be evaluated.

References

- [1] Amasaki, S. and Akashi, T.: Study on Measurement of Crack Depth of Concrete Member by Pulse Velocity Technique, Proceedings of JCI, Vol.2, pp.133-136, 1980. (in Japanese)
- [2] British Standard Institution: Recommendations for Measurements Velocity of Ultrasonic Pulses in Concrete, BS 1881, Part 203, pp.618-619, 1986.
- [3] Iwanami, M., Kamada, T. and Nagataki, S.: Application of Nondestructive Testing Methods for Evaluation of Material Deterioration in Concrete, Proceedings of JSNDI, Vol.46, No.3, pp.223-228, 1997. (in Japanese)
- [4] Akashi, T.: Studies on Nondestructive Testings of Concrete, Journal of JSCE, No.390/V-8, pp.1-22, 1988. (in Japanese)
- [5] Sato, H.: Theory of Elastic Waves, pp.20-38, 1988. (in Japanese)
- [6] Weng, G.J.: Some Elastic Properties of Reinforced Solids, with Special Reference to Isotropic Ones Containing Spherical Inclusions, International Journal of Engineering Science, Vol.22, pp.845-856, 1984.

- [7] Rayleigh, L.: The Theory of Sound, Vol.II, p152, 1929.
- [8] Mason, W.P. and McSkimin, H.J.: Attenuation and Scattering of High Frequency Sound Waves in Metals and Glasses, Journal of Acoustical Society of America, Vol.19, No.3, pp.464-473, 1947.
- [9] Kato, Y. and Uomoto, T.: Effect of Quantity and Specific Surface Area of Sand on Transition Zone of Cement Composites, Proceedings of JCI, Vol.20, No.2, pp.775-780, 1998. (in Japanese)
- [10] Miwa, S.: Theory of Powder Engineering, pp.5-10, 1991. (in Japanese)
- [11] Mindess, S.: Interfaces in Concrete, Materials Science of Concrete, pp.163-180, 1989.
- [12] Kuroda, M, Terashi, S. and Watanabe, T.: A Fundamental Study on Recycling Concrete, 50th Annual Convention of JSCE, Part V, pp.198-199, 1995. (in Japanese)
- [13] Kobayashi, K., Hattori, A., Miyagawa, T. and Fujii, M.: Characters of Interfacial Zone of Cement Paste with Additives around Aggregates, Journal of JSMS, Vol.45, No.9, pp.1001-1007, 1996. (in Japanese)